JOURNAL OF CATALYSIS 121, 31–46 (1990)

A Temperature-Programmed Reduction Study of Sulfided Co–Mo/Al_2O_3 Hydrodesulfurization Catalysts

B. SCHEFFER,[1] N. J. J. DEKKER, P. J. MANGNUS, AND J. A. MOULIJN[2]

Institute of Chemical Technology, University of Amsterdam, Nieuwe Achtergracht 166, 1018 WV Amsterdam, The Netherlands

Received June 2, 1988; revised June 7, 1989

The reduction of sulfided hydrodesulfurisation catalysts has been studied using temperature-programmed reduction of sulfides (TPR-S). Hydrogenation of stoichiometric sulfur of bulk Co_9S_8 and MoS_2 occurs at much higher temperatures than HDS operating temperatures and is thermodynamically limited under the TPR-S reduction conditions. Al_2O_3-supported Co and Mo catalysts contain sulfided species which are reduced at lower temperatures than bulk Co_9S_8 and MoS_2. In Co/Al_2O_3 catalysts with a high Co content Co_9S_8 is found, while a small amount of a CoS surface species is also present. High temperatures of calcination cause Co to migrate into the support, and this Co species remains oxidic during the sulfiding treatment. On Mo/Al_2O_3 catalysts it is found that around 600 K a sulfided Mo monolayer species is reduced. At higher temperature, reduction is observed of bulk-like MoS_2. In Co–Mo/Al_2O_3 catalysts the reduction of Mo occurs at nearly the same temperature as that of Mo/Al_2O_3. When the Co loading is low, no separate Co sulfide phase is detected, whereas catalysts with a high Co content contain Co_9S_8. A high temperature of calcination leads to the formation of nonsulfidable Co species. For all supported catalysts the TPR-S patterns indicate that some S is hydrogenated around 400 K. This S is chemisorbed on coordinatively unsaturated sites of Mo and Co sulfides when the H_2S pressure is sufficiently high, and it is hydrogenated at a lower H_2S/H_2 ratio. On Co/Al_2O_3 catalysts this S species is hydrogenated at a higher temperature than that of the corresponding species in Mo/Al_2O_3. On Co–Mo/Al_2O_3 a similar S species is found; it is hydrogenated at a lower temperature than that found for either Co/Al_2O_3 or Mo/Al_2O_3. This is an indication of the formation of a disperse Co–Mo species. The temperature of hydrogenation of the chemisorbed S species depends on the metal loading and the temperature of calcination. For all Co–Mo/Al_2O_3 catalysts, it is found that a low temperature of hydrogenation of S corresponds with a high HDS activity. It is concluded that the capacity to hydrogenate S, which is abstracted from S-containing compounds during the HDS reaction, is a key parameter for the overall HDS activity of Co–Mo/Al_2O_3 catalysts.

INTRODUCTION

Temperature-programmed reduction (TPR) is a valuable technique in the study of oxidic Mo/Al_2O_3 (*1*), Co/Al_2O_3 (*2*, *3*), and Co–Mo/Al_2O_3 (*4*) catalysts. Detailed information has been derived from TPR patterns concerning the nature and the amounts of the highly disperse species in these catalysts. In this way TPR has been used to clarify the effects of preparation parameters, such as metal loading and temperature of calcination, on the speciation of the final catalyst. Furthermore, it has been found that the HDS activity of sulfided catalysts can be rationalised to a large extent on the basis of the abundance of precursors in the oxidic catalysts (*5–8*). The sulfiding of Co/Al_2O_3 (*3*), Mo/Al_2O_3 (*9*) and Co–Mo/Al_2O_3 (*10*) catalysts has been studied using temperature-programmed sulfiding (TPS) and the sulfidability of the various oxidic species has been described in detail. Sulfidation causes drastic changes in the catalyst, and therefore it is worthwhile to subject the same catalyst samples to TPR in their sulfided form. To discriminate between TPR of oxidic and TPR of sulfided

[1] Present address: Koninklijke/Shell Laboratory, Badhuisweg 3, 1031 CM Amsterdam, The Netherlands.

[2] To whom correspondence should be addressed.

0021-9517/90 $3.00

samples, the latter technique will be abbreviated as TPR-S.

Compared with the spectroscopic techniques which have been applied to sulfided Co–Mo/Al_2O_3 catalysts TPR-S offers the following advantages:

—it is equally sensitive to disperse and to nondisperse species;
—reduction of all species is observed if the maximum temperature is high enough;
—the quantity of a species is easily obtained;
—it provides a measure of chemical reactivity which is closely related to catalytic activity.

TPR-S has previously been applied to Mo/Al_2O_3 (*11–13*), Co–Mo/Al_2O_3 (*11, 14*), and Ni–Mo/Al_2O_3 (*11, 13*). In all these studies the fraction of S in the catalysts which is hydrogenated in the TPR-S experiment is small (10–20%), because the maximum temperature reached was 870 K or lower. In the present work the maximum temperature was 1250 K, which is sufficiently high to completely reduce all Co and Mo species. Furthermore, the Co and Mo loadings and the temperatures of calcination were systematically varied. A comprehensive overview of the reduction behavior of sulfided Co–Mo/Al_2O_3 catalysts is thus obtained.

The TPR-S results of the sulfided Co–Mo/Al_2O_3 catalysts are interpreted on the basis of TPR-S results on bulk compounds, and relations between reducibility and HDS activity are discussed.

EXPERIMENTAL

Materials. MoS_2 (Pfalz & Bauer) and $CoSO_4 \cdot 7H_2O$ (Merck, p.a.) were used as supplied. Co_9S_8 was obtained by sulfiding Co_3O_4 (Merck, p.a.) up to 925 K.

Mo/Al_2O_3 catalysts were prepared via pore volume impregnation using solutions of $(NH_4)_6Mo_7O_{24} \cdot 6H_2O$. The catalysts were calcined in air at 825 K unless otherwise indicated. A detailed description of the preparation is given elsewhere (*9*).

To prepare the Co/Al_2O_3 catalysts the support was impregnated with aqueous solutions of $Co(NO_3)_2 \cdot 6(H_2O)$ followed by drying in air and heating in N_2 or calcining in air. Different Co loadings were obtained by using different concentrations of cobalt nitrate. Details are given elsewhere (*3*).

Co–Mo/Al_2O_3 catalysts were prepared starting from the Mo/Al_2O_3 samples (*4*); Co was added in the same way as for the Co/Al_2O_3 catalysts (*4*).

Catalysts will be designated by the number of metal atoms/nm^2, e.g. 1.6% CoO/10.2% MoO_3/Al_2O_3 as Co(0.8)Mo(2.5)/Al.

TPR-S. The TPR-S equipment consisted of a conventional TPR setup (*2*) to which a sulfiding apparatus was added for *in situ* sulfidation. A flow scheme of the TPR-S equipment is shown in Fig. 1. The sample was loaded in a quartz tube (inner diameter 4.5 mm) which was placed in an oven. The sample size was varied to adjust the H_2 consumption to 25–50 $\times$ 10^{-6} mol.

To measure H_2S a UV-spectrophotometer was used (Perkin–Elmer C75, set at 200 nm) which was equipped with a flow cell. H_2S has a strong absorption around 200 nm (*15*). The spectrometer was used in absorption mode so its signal was directly proportional to the H_2S concentration. H_2O and NO_x have only a weak absorption, but SO_2 (*16*) and NH_3 (*17*) may interfere with the H_2S signal. The detector was calibrated by the reduction of a known amount of MoS_2.

CH_4 formation was measured with a flame ionization detector (FID). The H_2

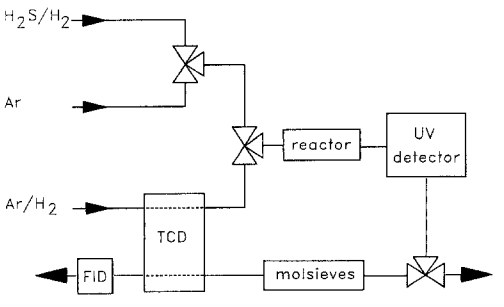

FIG. 1. Flow scheme of the TPR-S apparatus.

consumption was measured with a thermal conductivity detector (TCD) after H_2O and H_2S had been trapped in molecular sieves. In addition to the H_2 concentration, the TCD also detects NO, NO_2, and CH_4. NO and NO_2 can be produced during decomposition of the nitrates used in the preparation of the catalysts, and CH_4 can be formed during TPR from organic material which is adsorbed on the support from the laboratory atmosphere (*2*).

The amounts of H_2 consumed and H_2S produced were obtained by integration of the signals of the TCD and UV detectors respectively.

The procedure for sulfiding of the samples was as follows. The quartz reactor was first flushed with Ar (Matheson, UHP, purified through a BTS column) at room temperature to expel oxygen. The sulfiding gas (15.5% H_2S, balance H_2, Matheson) was next led through the reactor (15×10^{-6} mol/s, 1 bar) for 300 s at room temperature. Then the temperature was raised (0.16 K/s) to 675 K (or a different temperature where indicated). Sulfiding was continued at the maximum temperature for 1800 s. The sulfiding gas was subsequently replaced by Ar (37×10^{-6} mol/s), and after flushing for 2700 s the reactor was cooled to 300 K. During the sulfiding and flushing procedures the gases leaving the reactor were vented.

At the start of the TPR-S run the gas flow was switched to 67% H_2 in Ar as the reducing gas (15×10^{-6} mol/s, 1 bar) and the off-gas were led to the TPR equipment. The heating rate was 0.16 K/s up to 1250 K.

HDS activity. The activity of the catalysts for HDS of thiophene was measured in a microreactor under atmospheric pressure. Details of the activity measurements are given elsewhere (*5*).

RESULTS

Bulk Compounds

TPR-S patterns of bulk compounds are shown in Fig. 2. For the bulk sulfides no FID signal was observed. The H_2S production closely matched the H_2 consumption and no other products were detected.

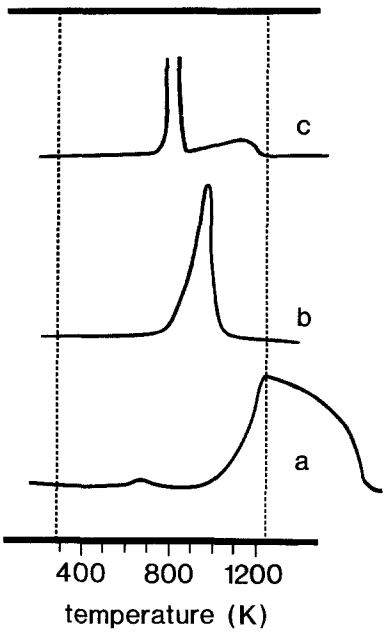

FIG. 2. TPR-S patterns of bulk compounds. (a) MoS_2, (b) Co_9S_8, (c) $CoSO_4 \cdot 7H_2O$. TCD signals are shown.

MoS_2. It is shown in Fig. 2a that reduction of bulk MoS_2 starts around 1000 K, and then the rate of reduction rises sharply. The rate of reduction is still rising when the maximum temperature of the TPR-S experiment (1250 K) is reached, so the maximum in the TPR-S pattern at 1250 K is an experimental artifact. Reduction continues in the isothermal stage for about 1500 s and then the rate of reduction rapidly drops. The total H_2 consumption during TPR-S indicates a degree of reduction of MoS_2 of around 90%. Possibly the sample contained Mo metal. A comparison of the TCD and UV signals shows that at approximately 700 K a small H_2 consumption occurs which is not coupled to H_2S production. This indicates that an oxygen-containing species was present in the sample.

Co_9S_8. To avoid reoxidation the sulfide was prepared by *in situ* sulfidation of Co_3O_4 at a maximum temperature of 925 K. Ac-

cording to TPS results Co_3O_4 is sulfided to Co_9S_8 at that temperature (*3*). Sulfidation of $Co(NO_3)_2 \cdot 6H_2O$ gave identical TPR-S results. Reduction of bulk Co_9S_8 (Fig. 2b) starts around 800 K, and a peak maximum is seen at 950 K. The total H_2 consumption is 1.1 H_2/Co.

$CoSO_4 \cdot 7H_2O$. The TPR-S pattern (Fig. 2c) shows two peaks, a sharp one at 790 K and a broader one at 1090 K. The shape and the position of the peak at high temperature are reminiscent of the TPR-S pattern of Co_9S_8, while the difference in temperature of reduction is likely to be caused by differences in particle size and sample size. It is therefore suggested that the sulfate is first reduced to the sulfide at 790 K. This is in accordance with the reported preparation of the sulfide from the sulfate by a treatment in H_2S/H_2 at 800 K (*18*).

Mo/Al_2O_3 Catalysts

The TPR-S pattern of a typical Mo/Al_2O_3 catalyst is shown in Fig. 3. No FID signal was observed. To facilitate the description, the TPR-S pattern is divided into three temperature regions:

region I: 300–550 K. A H_2 consumption peak is seen which is associated with a H_2S production peak.

region II: 550–1000 K. A continuous uptake of H_2 and a production of H_2S is seen, on which small shoulders are superimposed.

region III: 1000–1250 K. The rates of H_2 consumption and H_2S production rise sharply in this region and a maximum is observed.

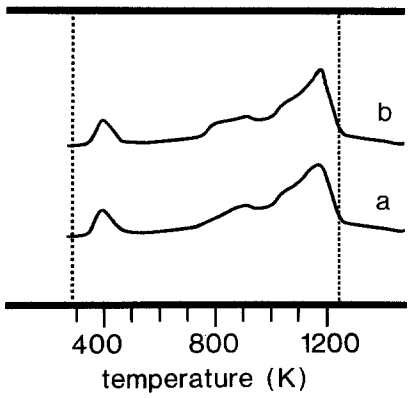

FIG. 3. TPR-S pattern of a $Mo(2.2)/Al_2O_3$ catalyst. UV signal (b) and TCD signal (a) are shown.

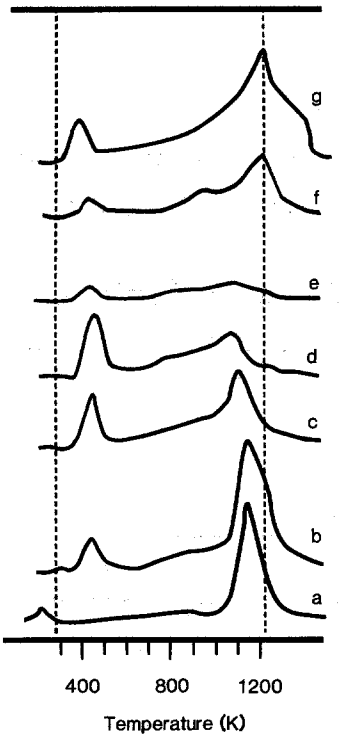

FIG. 4. TPR-S patterns (TCD signal) of Mo/Al_2O_3 catalysts calcined at 825 K. (a) Al_2O_3, (b) Mo(0.09)/Al, (c) Mo(0.2)/Al, (d) Mo(0.5)/Al, (e) Mo(1.8)/Al, (f) Mo(2.2)/Al, (g) Mo(4.5)/Al.

The total H_2S production in regions II and III is 1.85 S/Mo.

TPR-S patterns of Mo/Al_2O_3 catalysts with various loadings are shown in Fig. 4. For clarity only the TCD (H_2 consumption) signals are shown. Also included is a TPR-S pattern of the bare support after the regular sulfiding procedure (Fig. 4a). The support shows a small peak in region I and a sharp peak in region III (1150 K). The latter peak is attributed to cracking and reduction of impurities (sulfates) in the support (*2*). A similar reduction of impurities has been ob-

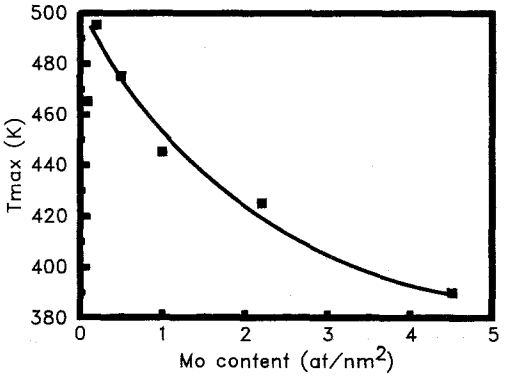

FIG. 5. Position of peak maximum in region I in TPR-S of Mo/Al_2O_3 catalysts.

served with oxidic samples in TPR (*3*) and TPS (*9*). The reduction of support impurities interferes most with the catalysts with the lowest Mo loadings (Mo(0.09)/Al and Mo(0.2)/Al).

The TPR-S patterns of the Mo/Al_2O_3 catalysts change as higher Mo loadings are applied:

—The peak in region I shifts from 475 to 390 K as the loading is increased, in accordance with previous results (*11*). This is shown more clearly in Fig. 5.

—The amount of H_2 consumed in region I per Mo atom decreases from 0.6 to 0.1 H_2/Mo toward higher loadings, as exemplified in Table 1.

—The relative importance of region II with respect to region III decreases as the loading is increased to Mo(4.5)/Al.

—With increasing loading the peak maximum in region III first shifts to lower temperatures, but from Mo(1.0)/Al to Mo(4.5)/Al it shifts to higher temperature again. The apparent shift found for the lowest loadings is caused by reduction of support impurities.

After correction for the reduction of support impurities (100×10^{-6} mol H_2/g Al_2O_3) the total H_2 consumption in regions II and III is 1.85 ± 0.2 H_2/Mo for all Mo catalysts studied (Table 1).

Co/Al_2O_3 Catalysts

Figure 6 shows TPR-S patterns of Co/Al_2O_3 catalysts which have been pretreated in different ways. For convenience the same division in temperature regions I–III is made as for that of the Mo/Al_2O_3 catalysts.

The Co/Al_2O_3 sample of Fig. 6a has been exposed to air at room temperature. The two-peak pattern strongly resembles the TPR-S pattern of $CoSO_4 \cdot 7H_2O$ (Fig. 2c). $CoSO_4 \cdot 7H_2O$ has been observed previously in air-exposed samples (*10*). Clearly it is essential to perform reduction of sulfided Co catalysts without prior exposure to the atmosphere.

Figures 6b–6c show the effect of the temperature of calcination on the TPR-S patterns of the Co(3.84)/Al catalysts. Table 2 shows amounts of H_2 which are consumed. After calcination at 825 K (Fig. 6b) H_2 consumptions are seen in regions I and II which are coupled to H_2S productions. The H_2S production in region II is 0.8 H_2S/Co. There is a shoulder on the TCD signal at 870 K due to reduction of adsorbed impurities. The reduction in region I appears to consist of two reduction peaks (465–490 K), both coupled with H_2S production (total 0.5 H_2S/Co). After calcination at 1025 K

TABLE 1

H_2 Consumption in TPR-S of Sulfided Mo/Al_2O_3 Catalysts

Mo content (at/nm²)	H_2 consumption	
	Region I	Region II + III
0.09	0.4	2.1
0.2	0.6	1.7
0.5	0.6	2.0
1.0	0.5	1.7
2.2	0.2	1.8
4.5	0.1	1.9

Note. All catalysts were calcined at 825 K. H_2 consumption is expressed as mol H_2/mol Mo. See text for the definitions of the temperature regions.

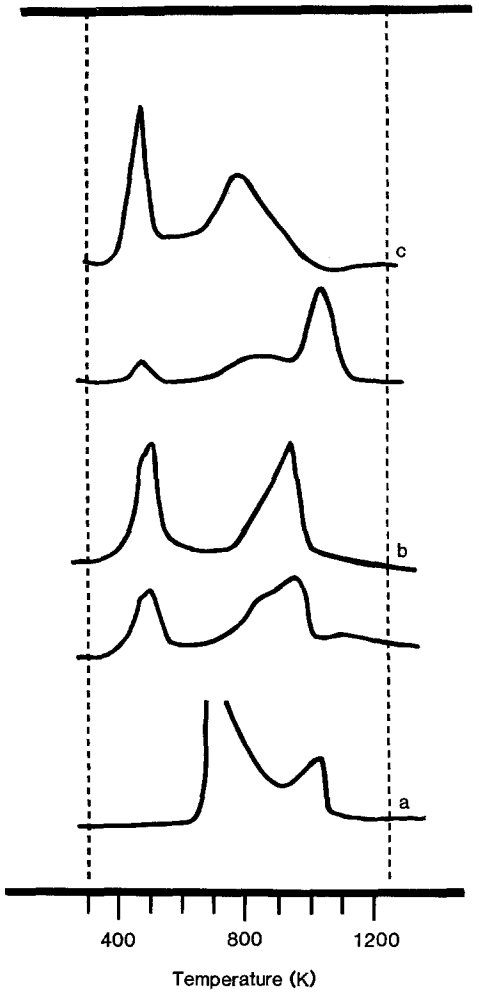

FIG. 6. TPR-S patterns of Co/Al_2O_3 catalysts. (a) Co/Al catalyst exposed to air before TPR-S; (b) Co(3.84)/Al calcined at 825 K; (c) Co(3.84)/Al calcined at 1025 K. UV signal (upper line) and TCD signal (lower line) are shown.

(Fig. 6c) the TPR-S pattern is markedly different:

—There is only a single small peak in region I (at 475 K).

—The H_2S production in region II is smaller (0.3 H_2S/Co).

—A H_2 consumption is seen in region III which is not associated with H_2S production.

Figure 7 shows the TPR-S patterns of Co(0.62)/Al catalysts which have been calcined at different temperatures. Because of the low Co content the TPR-S patterns are significantly disturbed by reduction of impurities in the support or adsorbed onto the support from the atmosphere after calcination.

TABLE 2

H_2 Consumption in TPR-S of Sulfided Co/Al_2O_3 Catalysts

Co content (at/nm²)	Calcination temperature (K)	H_2 consumption region		
		I	II	III
0.62	825	0.6	5.3[a]	0.4
0.62	1025	0.5	1.7[a]	0.7
3.84	825	0.4	1.2[a]	—
3.84	1025	0.1	0.5	0.6

[a] TPR-S pattern strongly influenced by reduction of adsorbed organics. H_2 consumption is expressed as mol H_2/mol Co. See text for the limits of the temperature regions.

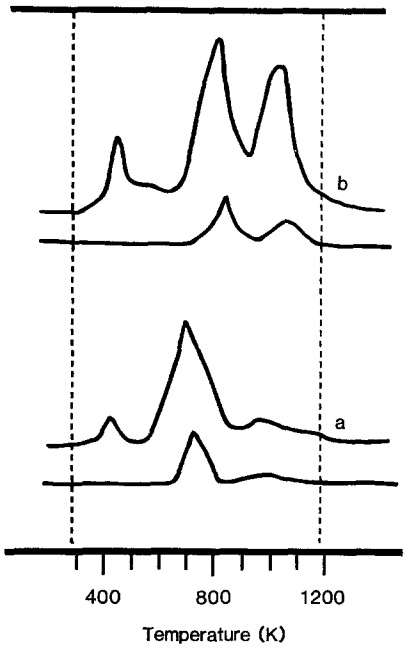

FIG. 7. TPR-S patterns of Co/Al_2O_3 catalysts. (a) Co(0.62)/Al calcined at 785 K; (b) Co(0.62)/Al calcined at 1025 K. TCD signal (upper line) and FID signal (lower line) are shown.

—After calcination at 825 K, a H_2 consumption and H_2S production (at 445 K) is seen in region I. In region II a large peak is seen which is associated with a signal of the FID detector indicating CH_4 formation. A large part of this peak is therefore due to reduction of adsorbed impurities, as has been found for the TPR of the oxidic catalysts as well (*2, 3*). A small TCD signal is seen in region III which is caused by reduction of impurities in the support.

—After calcination at 1025 K, H_2 consumption and H_2S production are found in region I at a higher temperature (480 K) than after calcination at 825 K. The signals from the FID and UV detectors in region II indicate that reduction of impurities occurs, as well as reduction of sulfided species. A large H_2 consumption is found in region III which is not related to a H_2S production.

The reduction of impurities renders the quantitative evaluation of region II in the TPR-S patterns of the Co(0.62)/Al samples unreliable. In region I differences are seen with the Co(3.84)/Al samples: after calcination at 825 K only single peaks are seen, and they occur at a lower temperature than those of the Co(3.84)/Al samples. After calcination at 1025 K no major differences are seen between catalysts with different loadings in region I.

Co–Mo/Al_2O_3 Catalysts

The TPR-S patterns of Co–Mo/Al_2O_3 catalysts calcined at 785 K are shown in Fig. 8. Also for these catalysts the patterns are conveniently divided into regions I–III:

—In region I a single peak of H_2 consumption and H_2S production (0.15 H_2S/Mo or 0.4 H_2S/Co) is seen for the Co(0.80)Mo/Al_2O_3 catalyst at a low temperature (355 K). At higher Co loadings a double peak is seen at 370/425 K for the Co(1.61)Mo/Al_2O_3 catalyst and at still higher temperatures (405/490 K) for the Co(4.07)Mo/Al_2O_3 catalyst; the H_2S production in region I increases to 0.21 and 0.29 H_2S/Mo, respectively.

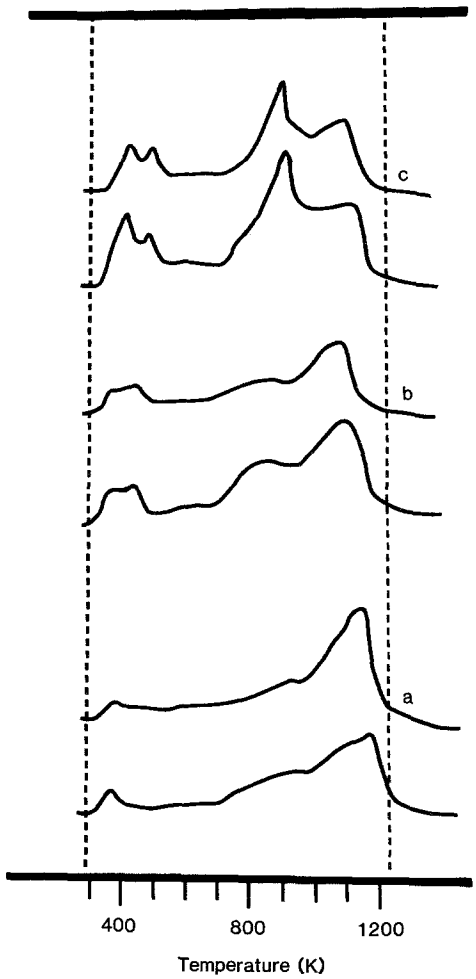

FIG. 8. TPR-S patterns of Co–Mo/Al_2O_3 catalysts calcined at 785 K. (a) Co(0.8)Mo/Al, (b) Co(1.61)Mo/Al, (c) Co(4.07)Mo/Al. UV signal (upper line) and TCD signal (lower line) are shown.

—In region II no clear peak is seen for the Co(0.80)Mo/Al_2O_3 catalyst. At higher loadings of Co a broad peak of H_2 consumption and H_2S production is observed, and at the highest loading a sharp peak has developed.

—In region III a H_2 consumption and H_2S production is seen similar to the TPR-S patterns of the Mo/Al_2O_3 catalysts.

The temperature of calcination also influences the TPR-S patterns strongly, as is

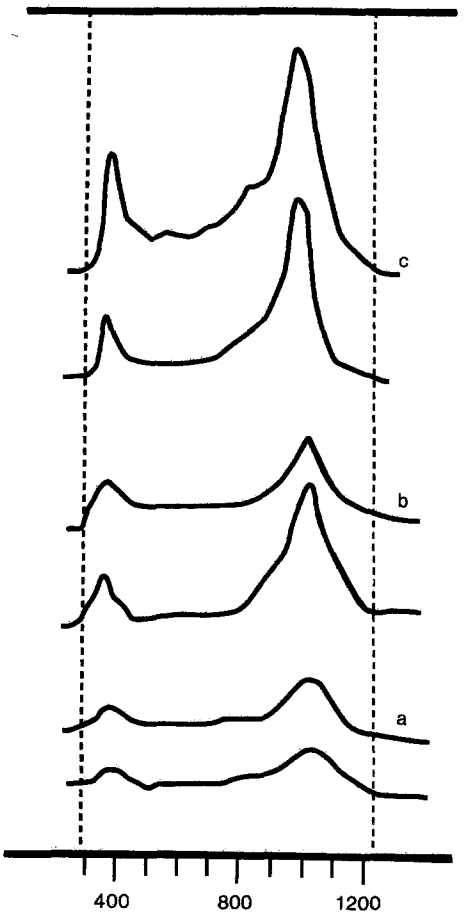

FIG. 9. TPR-S patterns of Co–Mo/Al_2O_3 catalysts calcined at 995 K. (a) Co(0.8)Mo/Al, (b) Co(1.61)Mo/Al, (c) Co(4.07)Mo/Al. UV signal (upper line) and TCD signal (lower line) are shown.

shown in Fig. 9 for catalysts calcined at 995 K:

—Only single peaks of H_2 consumption and H_2S production are seen in region I. Their size is not much influenced by the Co content.

—No peaks are seen in region II except for a shoulder at 810 K for the sample with the highest Co content.

—The peak in region III is somewhat shifted to lower temperature. The size of the H_2 consumption increases as the Co content is increased, and both the H_2 consumption and the H_2S production peak become sharper.

The quantitative TPR-S results are given in Table 3. Except for the values referring to region II, the H_2 consumption is expressed as H_2/Mo since the Mo content is constant while the Co content is varied.

DISCUSSION

Bulk Compounds

It is instructive to compare the TPR results on oxidic samples with the TPR-S results on sulfided samples. The reduction of MoS_2 occurs at a much higher temperature than the reduction of MoO_3; the reduction of MoS_2 only starts at 1000 K, while MoO_3 is already extensively reduced at that temperature (*19*). It has been found that the reduction of MoO_3 to MoO_2 is kinetically controlled under the present conditions, while the reduction of MoO_2 to Mo metal is controlled by thermodynamic limitations, viz., by the H_2O/H_2 ratio at which Mo metal is thermodynamically stable (*19*). Since H_2S is thermodynamically less stable than H_2O (*20*), the reduction of MoS_2 is even more likely to be thermodynamically controlled.

TABLE 3

H_2 Consumption in TPR-S of Sulfided Co–Mo/Al_2O_3 Catalysts

Co content (at/nm²)	Calcination temperature (K)	H_2 consumption region		
		I	II	III
0.80	785	0.2	—	2.2
0.80	995	0.5	—	2.2
1.61	785	0.3	0.3*	2.1
1.61	995	0.3	—	2.1
4.07	795	0.5	0.3*	2.7
4.07	995	0.5	—	2.7
				3.7

Note. All catalysts have a Mo content of 2.49 at/nm². H_2 consumption is expressed as mol H_2/mol Mo. H_2 consumptions in regions II and III were added, except for entries marked *, where H_2 consumption in the deconvoluted peak is expressed as mol H_2/mol Co. See text for the limits of the temperature regions.

To verify this point the H_2S/H_2 ratio at which MoS_2 is in equilibrium with Mo metal was calculated, based on the free enthalpies of formation of the relevant compounds (*20*). The actual H_2S/H_2 ratios at different temperatures during the TPR-S experiment were calculated from the TPR-S patterns. Figure 10 shows that in general the actual H_2S/H_2 ratios are lower than the thermodynamic values, but above 1000 K they approach the equilibrium values; the difference is ca. 40% at the highest temperature, and this can well be explained by a concentration gradient of H_2S across the particles. The H_2S pressure within the MoS_2 particles is higher than the average gas-phase pressure because of slow diffusion of H_2S out of the particles. Also in TPS of MoO_3 it has been found that H_2S diffusion is slower than H_2 diffusion (*9*). It is therefore concluded that the differences observed are due to mass transfer limitations, and essentially the reduction of MoS_2 is thermodynamically limited under the TPR-S conditions.

In TPR-S of MoS_2 no reduction is observed below 1000 K. This contrasts with results which have been obtained on MoS_2 samples which are prepared from the decomposition of thiosalts (*21, 22*). These preparations have high surface areas and contain nonstoichiometric sulfur up to a ratio of S/Mo of 2.5. When reduction is carried out up to 700 K the S/Mo ratio approaches 2, in agreement with the present results, so reduction below 700 K is clearly related to nonstoichiometric S. The MoS_2 sample studied here only contains stoichiometric sulfur, so clearly the abundance of nonstoichiometric sulfur species depends on the method of preparation (*23*).

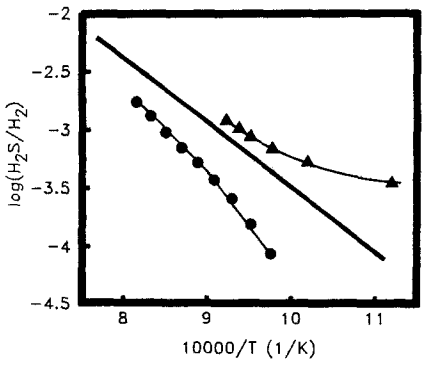

FIG. 10. Comparison of actual H_2S/H_2 ratio during TPR-S of MoS_2 (●) and Mo/Al_2O_3 (▲) with the H_2S/H_2 ratio of thermodynamic equilibrium of MoS_2 with Mo metal (straight line).

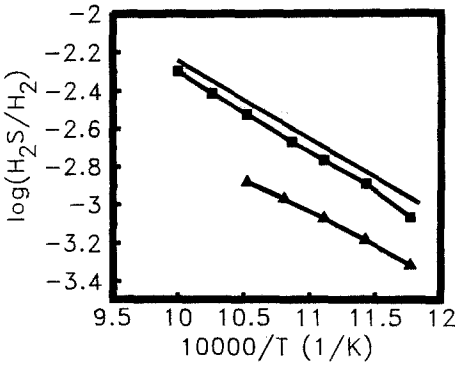

FIG. 11. Comparison of actual H_2S/H_2 ratio during TPR-S of Co_9S_8 (■) and Co/Al_2O_3 (▲) with the H_2S/H_2 ratio of thermodynamic equilibrium of Co_9S_8 with Co metal (straight line).

The reduction of Co_9S_8 occurs at a much higher temperature than the reduction of Co_3O_4 (cf. Ref. (*2*)). A thermodynamic limitation on the reduction was verified in a way similar to the procedure used for MoS_2. The result is shown in Fig. 11. Taking into account the experimental error and the uncertainties in the thermodynamic properties at these high temperatures, it is clear that the experimental H_2S/H_2 ratios are so close to thermodynamic equilibrium that the reduction of Co_9S_8 is also thermodynamically controlled. This is corroborated by the peculiar shape of the peak in TPR-S, viz., an exponential increase in the rate of reduction and a sudden halt to the reduction. Typical TPR peaks for kinetically controlled reductions are in general more symmetrical.

The reduction pattern of $CoSO_4 \cdot 7H_2O$ differs widely from the patterns of Co and Mo sulfides, so the sulfate can be easily identified by TPR-S in samples of unknown composition. The sharpness of the peak at

790 K indicates that thermodynamic inhibition of reduction is absent, while the large width of the peak at 1090 K is indicative of thermodynamic control. Since the reduction of sulfate to sulfide is not thermodynamically controlled, the widths of the peaks confirm that $CoSO_4$ is first reduced to Co_9S_8 and subsequently reduced to Co metal at a higher temperature.

Mo/Al_2O_3 Catalysts

The TPR-S results confirm that Mo/Al_2O_3 catalysts are extensively sulfided at a common sulfiding temperature of 675 K. Temperatures in excess of 1000 K are required to fully reduce sulfidic Mo/Al_2O_3 catalysts. The reduction peak in region III, which is found for the supported catalysts, is also seen in the TPR-S of bulk MoS_2. In Fig. 10 the actual H_2S/H_2 ratio during TPR-S is compared with the thermodynamic equilibrium ratios and it is seen that at high temperatures the thermodynamic ratio is approached. Therefore at high temperature (region III) the reduction of Mo/Al_2O_3 catalysts is thermodynamically limited. This is also similar to bulk MoS_2, and it is concluded that the reduction in region III is due to the reduction of a MoS_2-like species in the catalyst. This is corroborated by the increase of the peak in region III as the Mo loading is increased, indicating that the Mo/Al_2O_3 catalysts more and more resemble bulk MoS_2. This agrees with the detection of single-slab MoS_2 particles in Mo/Al_2O_3 catalysts (*24–27*). The accompanying H_2S production is caused by the hydrogenation of stoichiometric sulfur.

The reduction in region II is not present in TPR-S of bulk MoS_2. Figure 10 indicates that the H_2S/H_2 ratio in region II is higher than the equilibrium ratio. According to thermodynamics this implies that MoS_2 cannot be reduced to Mo metal. The reduction of other Mo bulk sulfides can also be excluded: MoS_3 is not formed in H_2S at 675 K (*28*), and the presence of Mo_2S_3 is unlikely because the formation of Mo_2S_3 from MoS_2 is slow at these temperatures (*25*). The reduction in region II is therefore assigned to the hydrogenation of a S species which is more labile than stoichiometric sulfide sulfur. The lability of the S species indicates that the Mo species in which it is located contains many defects or is destablished through interaction with the support. Possibly this species consists of Mo ions in a monolayer MoS_2 surface species (*9, 29, 30*). Such species are not as stable as crystalline MoS_2, so their reduction is not in conflict with the thermodynamic limitation of MoS_2 reduction.

In region I Hydrogenation of a S species which has been called S_x (*12*) is observed. In previous TPR-S experiments (*11, 12*) a maximum temperature has been applied which is too low to cause hydrogenation in regions II and III, so the peak in region I is the only peak maximum which has been reported up to now. Stuchlý and Klusácek (*14*) found a similar peak at a higher temperature (600 K). The peak is most probably shifted because they applied a much lower H_2 pressure (0.01 bar (*14*)). Peaks in region I are not reported by Burch and Collins (*13*), which is possibly due to the low resolution of their TPR-S patterns.

The peak in region I in the TPR-S pattern of this work is sharp and is found at a relatively low temperature. This indicates that S_x is a well-defined and highly reactive species. S_x is not to be equated with elemental sulfur because it has been shown that elemental sulfur is catalytically hydrogenated in a H_2S/H_2 atmosphere at 550 K over Mo/Al_2O_3 catalysts during sulfiding (*9*). As a consequence there can be no elemental sulfur present in the samples, even if sulfur were not evaporated during the Ar flush. From Fig. 10 it can be deduced that MoS_2 cannot be reduced at this temperature, so S_x is neither stoichiometric sulfur nor elemental sulfur. The S_x species is formed from H_2S during sulfiding in H_2S/H_2 and hydrogenated in pure H_2. This means that its presence depends strongly on the H_2S/H_2 ratio in the gas phase. The above characteristics indicate that S_x consists of chemi-

sorbed S, formed by H_2S decomposition on Mo sulfide species. Also on noble metal catalysts used for reforming S chemisorption plays an important role (*31*). It is well known that O_2 chemisorbs on MoS_2 (*29, 32, 33*). O_2 chemisorption has also been reported for sulfided Ni (*34*) and Fe (*35*), and likewise the formation of chemisorbed S is not restricted to MoS_2; hydrogenation of similar S_x species has recently been observed for sulfided Co (vide infra), Ni, Fe, W, and V (*36*).

O_2 and NO chemisorption preferentially occur on coordinatively unsaturated sites (*29, 32, 33*). For unsupported MoS_2 the coordinatively unsaturated sites reside on the edges of the MoS_2 slabs and not on the basal planes (*23–25, 26, 32, 33*). In view of the similarity of the sulfided Mo species with MoS_2, S_x is identified as S chemisorbed on the edges and corners of the MoS_2 slabs. Since the S_x/Mo ratio exceeds the number of corner sites for all but the smallest particle sizes (*23*), the edges are identified as the major adsorption sites.

It follows from the simple model of the MoS_2 structure (*23*) that most of the S atoms on edge and corner positions are nonstoichiometric; i.e., they are present in excess of a S/Mo ratio of 2. Their removal therefore generates coordinatively unsaturated sites, but does not involve the reduction of Mo^{4+} ions. The present TPR-S results are in accordance with this model since the amount of S hydrogenated in regions II and III is close to the stoichiometric amount, and S_x is clearly present in excess of the stoichiometric amount. The conclusions regarding the structures of the sulfidic species which are reduced in regions I, II, and III during TPR-S agree well with recent findings based on isothermal reduction studies of a MoS_2/Al_2O_3 catalyst (*37*).

The fraction of edge sites and the size of the MoS_2 crystallites are inversely related (*23*). The S chemisorption can therefore be used to estimate the dispersion of the Mo sulfide species. When the temperature of sulfiding is fixed, it follows from the TPR-S results that the dispersion of Mo decreases as the Mo loading is increased (Table 1). This is in accordance with results derived by other techniques (*24, 29*).

The position of the S_x peak in region I is a possible indication of the strength of chemisorption. From Fig. 5 it is clear that S chemisorption is strongest at low loadings of Mo. This shows that not only the dispersion but also the nature of the Mo sulfide species changes as the Mo loading is varied. This change can be an effect of the small size of the crystallites or it can result from the interaction with the support, since it is known that the interaction is relatively stronger for low Mo loadings (*1, 4, 6, 9*).

Co/Al_2O_3 Catalysts

From a comparison of Figs. 2b and 6b–6c it is clear that the catalysts with the high Co loading contain a species which is similar to Co_9S_8 (cf. (*3, 7, 38*)). This is confirmed in Fig. 11 where it is shown that the actual H_2S/H_2 ratio during TPR-S approaches the thermodynamic equilibrium ratio, as was also found for bulk Co_9S_8. The peak in region II is therefore ascribed to hydrogenation of stoichiometric sulfide S from Co_9S_8.

For the catalysts with the low loading the TPR-S pattern is difficult to interpret because of the relatively large signals due to reduction of organic impurities. It is interesting to note that in TPR of the oxidic sample reduction of organic impurities is also observed but to a much smaller extent (*2, 3*). This does not mean that the oxidic samples are less contaminated, but it is rather due to the catalytic effect of Co species on hydrogenation of adsorbed organics (*2*): in the oxidic catalysts Co species are extremely difficult to reduce, and oxidic species are poor catalysts for the hydrogenation of the adsorbed organics. Therefore the organics are cracked at a higher temperature instead. The TPR-S results on the same catalysts show that Co is sulfidable, and the sulfided Co species are reduced at a much lower temperature than the oxidic

species. Since both Co metal and Co sulfides catalyse hydrogenation of the organics, large H_2 consumptions are observed at lower temperatures.

Analogous to the Mo/Al_2O_3 catalysts, the hydrogenation which is seen in region I is not due to elemental S because Co_9S_8 is an excellent catalyst for the hydrogenation of S (*39*), and elemental S is expected to be hydrogenated during the sulfiding pretreatment. The reduction of stoichiometric S from Co_9S_8 is excluded on thermodynamic grounds, and since the phenomenon is very similar to the effects seen for Mo/Al_2O_3, the peaks in region I are also ascribed to hydrogenation of chemisorbed sulfur. Bulk Co_9S_8 does not have the slab-like structure of MoS_2, so the TPR-S patterns show that the formation of chemisorbed sulfur (S_x) is not restricted to specific edge or corner sites. In general S chemisorption occurs on coordinatively unsaturated sites which are present at the surface of highly disperse species.

The temperature at which hydrogenation of S_x occurs is in general higher than that seen with Mo/Al_2O_3 catalysts. This is probably caused by a stronger chemisorption and not by an intrinsic catalytic effect, because Co_9S_8 is an even better catalyst for S hydrogenation than MoS_2 (*39*).

An indication for a CoS surface phase (*3, 38*) is found in region I, where for some catalysts two maxima are observed: they are ascribed to hydrogenation of excess S from Co_9S_8 and from CoS, respectively.

The effect of a high temperature of calcination is clearly shown in the TPR-S results. After calcination at 1025 K sulfided species are present, but also reduction of an oxidic Co species is seen in region III, and the amount of Co which is sulfided is smaller. This agrees well with TPS results obtained on the same samples (*3*). From TPR on oxidic samples it is known that a dilute spinel phase is formed in these catalysts through diffusion of Co ions into the support (*2*). TPS experiments showed that this species is sulfided at 1000 K (*3*). Evidently back-diffusion of Co ions to the surface of the support does not occur at the temperature of the sulfiding treatment applied here. This is in accordance with the kinetic model for solid-state diffusion which has been derived for the diffusion of Ni ions in Al_2O_3 (*40*).

Co–Mo/Al_2O_3 Catalysts

The general features of the TPR-S patterns of the $Co–Mo/Al_2O_3$ catalysts are similar to patterns of Co/Al_2O_3 or Mo/Al_2O_3 catalysts. The reduction occurring in region III is therefore largely attributed to hydrogenation of S from MoS_2-like species. After calcination at 995 K the pattern of the $Co–Mo/Al_2O_3$ catalysts differs from that of the Mo/Al_2O_3 catalysts. This is of course due to the presence of the diluted Co spinel species in region III, in agreement with TPS results (*10*). This accounts for the changes in H_2 consumption since the Co spinel phase is oxidic, but it is remarkable that changes are also seen in the H_2S production. No Co sulfide species are reduced in region III, and the high-temperature side of the MoS_2 reduction peak has disappeared, so it is concluded that the reduction of sulfided Mo is accelerated by the reduction of the Co spinel phase. An explanation for this phenomenon is that the Co ions diffuse from the bulk of the support to the surface, because obviously reduction only occurs at the surface. As the Co ions reach the surface they break up the sulfidic Mo species, creating defects where reduction of Mo occurs. H_2 spillover from reduced Co may also increase the rate of reduction of sulfided Mo.

When the Co loading is high in supported catalysts, reduction is seen in region II. This is ascribed to crystalline Co_9S_8 because in TPR-S of unsupported Co_9S_8 reduction is observed in this region.

Interesting differences between $Co–Mo/Al_2O_3$ and Co/Al_2O_3 or Mo/Al_2O_3 are seen in region I. For the catalysts calcined at 785 K hydrogenation of the S_x species occurs at

a temperature which is lower than in the case of either Co/Al_2O_3 or Mo/Al_2O_3. This effect is already clearly seen for the lowest Co loading. At higher Co loadings a double peak is seen. This shows that at higher loadings a separate Co species is formed, while a limited amount (2 wt.% CoO) of Co forms a phase with Mo. This is confirmed by the absence of separate peaks in region II originating from the reduction of Co_9S_8 for Co–Mo/Al_2O_3 catalysts with low Co loadings. This also suggests that Co is incorporated in a different phase, viz., a Co–Mo species. This conclusion agrees well with the observation of Co_9S_8 in catalysts with a high loading (*10*), while the formation of a Co–Mo phase ("CoMoS") is generally reported (*1, 5, 7, 10, 24, 26, 41*).

The temperature of the peak maximum in region I shows that the chemisorption of S on the Co–Mo phase is weaker than that on the monometallic Co and Mo species. The hydrogenation in region I serves as an indicator for the formation of a Co–Mo species and it can be seen that it is present after calcination at 785 K. After calcination at 995 K the peak in region I resembles the peak in Mo/Al_2O_3, which indicates that the Co–Mo phase is not present. The effects of Co loading and temperature of calcination on the formation of the sulfided Co–Mo phase are in complete agreement with the trends observed for the oxidic Co–Mo phase (the CoMoS precursor) on the basis of TPR on oxidic Co–Mo/Al_2O_3 catalysts (*4, 5, 8*). This corroborates that interaction of Co and Mo in sulfided catalysts originates in the oxidic precursor; i.e., the Co–Mo phase is not formed from separate Co and Mo species during sulfiding of the catalysts.

It has been shown that the chemisorption of S occurs on the edges of MoS_2 crystallites. The strong effect of Co (in the Co–Mo species) on S chemisorption strongly suggests that Co is also located at or near the edges. This position of Co is supported by results of other techniques as well (*24, 26, 33*).

Relation of S chemisorption to HDS Activity

The S_x species is shown to consist of S adsorbed on coordinatively unsaturated sites of Co and Mo species. The coordinatively unsaturated sites are essential for the catalytic activity, and for Mo/Al_2O_3 catalysts a correlation has been found between the amount of O_2 chemisorption and the HDS activity (*29, 32, 42*). A correlation between the total amount of H_2S produced in TPR-S up to 775 K and the HDS activity of Ni–Mo/Al_2O_3 catalysts has also been reported (*13*). It is therefore of interest to consider a possible correlation between the formation of the S_x species and catalytic activity. The HDS activities of most of these samples have been reported elsewhere (*5, 6*). In Fig. 12 the amount of S_x which is hydrogenated is compared with the HDS activity of Mo/Al_2O_3 catalysts. The catalysts were sulfided at 675 K before TPR-S and before the catalytic test. It is seen that both the HDS activity and the amount of S_x increase as the Mo loading is increased, but at loadings higher than 8% MoO_3 the S chemisorption does not increase further while the activity continues to rise. It has been found that O_2 chemisorption on Mo/Al_2O_3 catalysts shows the same behaviour (*29, 32, 42*).

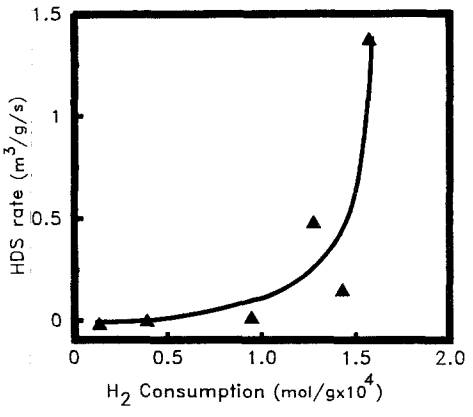

FIG. 12. Relation between the amount of H_2 consumption in region I during TPR-S and the HDS activity for Mo/Al_2O_3 catalysts.

The TPR-S experiments not only allow the determination of the quantity of adsorbed S but they also give an indication of the ability of the catalysts to hydrogenate the adsorbed S, by a consideration of the temperature of the peak maximum of S_x hydrogenation. For comparison the activity of the catalysts is expressed as the rate of thiophene removal per Mo atom present in the catalyst. In Fig. 13 the HDS activity of Mo/Al_2O_3 catalysts is plotted vs the position of the peak in region I in TPR-S. It is clear that a high HDS activity is associated with a low temperature of the peak maximum. This indicates that the activity for S_x hydrogenation of a Mo/Al_2O_3 catalyst parallels the activity for HDS. This is an interesting result because the formation of the S_x species in a H_2S/H_2 mixture and its hydrogenation in H_2 occur at temperatures at which the HDS reaction is catalysed. This means that during HDS a S_x species may be present when a sufficiently high H_2S/H_2 ratio is reached. It is likely that S_x acts as a poison by blocking the coordinatively unsaturated sites, and therefore it is understandable that the rate of hydrogenation of S_x strongly influences the HDS rate.

The correlation between rate of S_x hydrogenation and HDS activity also holds for the Co/Al_2O_3 catalysts. The temperature of S_x hydrogenation on Co/Al_2O_3 is higher, and, as expected, the activity of Co lower than that found for the Mo/Al_2O_3 catalysts.

The $Co–Mo/Al_2O_3$ catalysts also illustrate that the S_x hydrogenation activity is essential for HDS. The $Co–Mo/Al_2O_3$ catalysts which show a single peak in region I at low temperature are the most active catalysts. Compared with Mo/Al_2O_3 the temperature of the peak maximum in region I is lower and the HDS activity higher. It therefore seems that the Co–Mo species is an excellent catalyst for both S_x hydrogenation and HDS. The appearance of a second peak in region I for catalysts with a high Co content signals the segregation of Co out of CoMoS into Co_9S_8. Indeed the activity of those catalysts is lower since Co_9S_8 is much less active (*26*).

It is tempting to relate the rate of S_x hydrogenation to the strength of chemisorption of S. An optimal Me–S bond strength is predicted on the basis of classical catalytic theory, and the synergistic effect of Co and Mo has been explained by the formation of S species with a bond strength intermediate between Co and Mo sulfide species (*43*). However, the present results show that the rate of hydrogenation of S_x is higher for $Co–Mo/Al_2O_3$ than for both Co/Al_2O_3 and Mo/Al_2O_3. Furthermore, there is a monotonic increase in activity as the S_x species is hydrogenated at lower temperature. This suggests that the Me–S bond strength in the CoMoS species is lower than that in Co and Mo species.

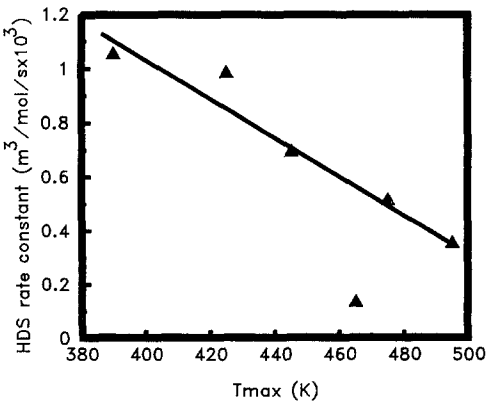

FIG. 13. Relation between the temperature of H_2 consumption in region I during TPR-S and HDS activity for Mo/Al_2O_3 catalysts.

CONCLUSIONS

Temperature-programmed reduction of sulfides has been successfully used to elucidate the nature of sulfidic species on $Co–Mo/Al_2O_3$ catalysts. The reduction of bulk Co and Mo sulfides is more difficult than the reduction of the corresponding oxides. Under the TPR-S conditions the reduction of bulk Co_9S_8 and MoS_2 is thermodynamically controlled.

In TPR-S of Al_2O_3-supported catalysts reduction starts at lower temperatures than those found for the bulk sulfides, due to the

high concentration of defects in the surface compounds. In Co/Al_2O_3 catalysts there are indications of the presence of a highly disperse sulfided Co species ("CoS"). Catalysts with a high Co content also contain Co_9S_8. Calcination at high temperatures causes the diffusion of Co into the Al_2O_3 support. TPR-S shows that these Co species remain oxidic during practical sulfiding treatments at 675 K.

In TPR-S of Mo/Al_2O_3 samples the reduction of MoS_2-like species is observed at high temperatures. At lower temperature the reduction is seen of a sulfided Mo monolayer species.

Except for the peak at low temperature the TPR-S patterns of Co–Mo/Al_2O_3 catalysts are similar to those of Co/Al_2O_3 and Mo/Al_2O_3, but at high temperatures Mo species are somewhat easier to reduce than in Mo/Al_2O_3.

It has been found that during sulfiding considerable amounts of S are chemisorbed on Co and Mo species. When the H_2S/H_2 ratio is low the hydrogenation of this chemisorbed S is observed in TPR-S. By analogy with O_2 chemisorption the S chemisorption is considered to occur on coordinatively unsaturated sites. This is confirmed by the correlation which has been established between the chemisorption of S and the HDS activity: catalysts from which chemisorbed S is hydrogenated at lower temperature display the higher HDS activity. This correlation extends to Co–Mo/Al_2O_3 catalysts as well: the temperature of hydrogenation is lower than in either Co/Al_2O_3 or Mo/Al_2O_3 and the HDS activity is higher. This TPR-S result is a confirmation of the formation of a mixed sulfided Co–Mo species which differs from Co and Mo sulfides.

REFERENCES

1. Thomas, R., de Beer, V. H. J., and Moulijn, J. A., *Bull. Soc. Chim. Belg.* **90,** 1349 (1981).
2. Arnoldy, P., and Moulijn, J. A., *J. Catal.* **93,** 38 (1985).
3. Arnoldy, P., de Booys, J. L., Scheffer, B., and Moulijn, J. A., *J. Catal.* **96,** 122 (1985).
4. Arnoldy, P., Francken, M. C., Scheffer, B., and Moulijn, J. A., *J. Catal.*/ **96,** 381 (1985).
5. Scheffer, B. van Oers, E. M., Arnoldy, P., de Beer, V. H. J., and Moulijn, J. A., *Appl. Catal.* **25,** 303 (1986).
6. Thomas, R., van Oers, E. M., de Beer, V. H. J., Medema, J., and Moulijn, J. A., *J. Catal.* **76,** 241 (1982).
7. Wivel, C., Candia, R., Clausen, B. S., Morup, S., and Topsøe, H., *J. Catal.* **68,** 453 (1981).
8. Topsøe, N.-Y., and Topsøe, H., *J. Catal.* **77,** 293 (1982).
9. Arnoldy, P., van den Heijkant, J. A. M., de Bok, G. D., and Moulijn, J. A., *J. Catal.* **92,** 35 (1985).
10. Scheffer, B., de Jonge, J. C. M., Arnoldy, P., and Moulijn, J. A., *Bull. Soc. Chim. Belg.* **93,** 751 (1984).
11. Nag, N. K., Fraenkel, D., Moulijn, J. A., and Gates, B. C., *J. Catal.* **66,** 166 (1980).
12. Ramachandran, R., and Massoth, F. E., *Canad. J. Chem. Eng.* **60,** 17 (1982).
13. Burch, R., and Collins, A., *Appl. Catal.* **18,** 373 (1985).
14. Stuchlý, K., and Klusácek, K., *Appl. Catal.* **34,** 263 (1987).
15. Stevenson, D. P., Coppinger, G. M., and Forbes, J. W., *J. Amer. Chem. Soc.* **83,** 4350 (1961).
16. Duerig, H., *Vib. Spectra Struct.* **12,** 193 (1983).
17. Nakayama, T., Kitamura, M. Y., and Watanaba, K., *J. Chem. Phys.* **30,** 1180 (1959).
18. Pasquariello, D. M., Kershaw, R., Passaretti, J. D., Dwight, K., and Wold, A., *in* "Solid State Chemistry in Catalysis" (R. K., Grasselli, J. F. Brazdil, Eds.), ACS Symposium Series **279,** p. 247. Amer. Chem. Soc., Washington, DC, 1985.
19. Arnodly, P., de Jonge, J. C. M., and Moulijn, J. A., *J. Phys. Chem.* **89,** 4517 (1985).
20. Barin, I., and Knacke, O., "Thermochemical Properties of Inorganic Substances." Springer-Verlag, Berlin (1973).
21. Kalthod, D. G., and Weller, S. W., *J. Catal.* **95,** 455 (1985).
22. Dianis, W. P., *Appl. Catal.* **30,** 99 (1987).
23. Farragher, A. L., and Cossee, P., *in* "Proceedings, 5th International Congress on Catalysis, Palm Beach, 1972" (J. Hightower, Ed.), p. 1301. North-Holland, Amsterdam, 1973.
24. Candia, R., Sorensen, O., Villadsen, J., Topsøe, N.-Y., and Clausen, B. S., *Bull. Soc. Chim. Belg.* **93,** 763 (1984).
25. Furimsky, E., *Catal. Rev. Sci. Eng.* **22,** 371 (1980).
26. Topsøe, H., and Clausen, B. S., *Appl. Catal.* **25,** 273 (1986).
27. Topsøe, N.-Y., Topsøe, H., Sorensen, O., Clausen, B. S., and Candia, R., *Bull. Soc. Chim. Belg.* **93,** 727 (1984).
28. Fukuda, K., Dokiya, M., Kameyama, T., and Kotera, Y., *Ind. Eng. Chem. Fundam.* **17,** 243 (1978).

29. Bachelier, J., Tilette, M. J., Duchet, J. C., and Cornet, D., *J. Catal.* **76,** 300 (1982).
30. Chung, K. S., and Massoth, F. E., *J. Catal.* **64,** 320 (1982).
31. Menon, P. G., and Prasad, J., *in* "Proceedings, 6th International Congress on Catalysis, London, 1976" (G. C. Bond, P. B. Wells, F. C. Tompkins, Eds.), p. 1061. The Chemical Society, London, 1977.
32. Tauster, S. J., Pecoraro, T. A., and Chianelli, R. R., *J. Catal.* **63,** 515 (1983).
33. Topsøe, N.-Y., and Topsøe, H., *J. Catal.* **84,** 386 (1983).
34. Bachelier, J., Duchet, J. C., and Cormet, D., *J. Phys. Chem.* **84,** 1925 (1980).
35. Groot, C. K., Ph.D. thesis, Eindhoven University of Technology, 1985.
36. Mangnus, P. J., Scheffer, B., and Moulijn, J. A., to be published.
37. Wambeke, A., Jalowiecki, L., Kasztelan, S., Grimblot, J., and Bonnelle, J. P., *J. Catal.* **109,** 320 (1988).
38. Chung, K. S., and Massoth, F. E., *J. Catal.* **64,** 332 (1982).
39. Zazhigalov, V. A., Gerei, S. V., and Rubanik, M. Ya., *Kinet. Katal.* **16,** 967 (1975).
40. Scheffer, B., Heijinga, J. J., and Moulijn, J. A., *J. Phys. Chem.* **91,** 4752 (1987).
41. Topsøe, H., Clausen, B. S., Candia, R., and Wivel, C., *Bull. Soc. Chim. Belg.* **90,** 1189 (1981).
42. Vissers, J. P. R., Bachelier, J., ten Doeschate, H. J. M., Duchet, J. C., de Beer, V. H. J., and Prins, R., *in* "Proceedings, 8th International Congress on Catalysis, Berlin, 1984," p. 387. Verlag-Chemie, Weinheim, West Berlin, 1984.
43. Harris, S., and Chianelli, R. R., *J. Catal.* **86,** 400 (1984).